Estradiol Enhances the Resistance of LDL to Oxidation by Stabilizing apoB-100 Conformation†

Roberto Brunelli,‡ Giampiero Mei,§ Ewa K. Krasnowska,|| Flavia Pierucci,⊥ Lucio Zichella,‡ Fulvio Ursini,# and Tiziana Parasassi*,||

I and II Clinica Ostetrica e Ginecologica, Universitá di Roma La Sapienza, Viale del Policlinico 155, 00185 Roma, Italy, and Dipartimento di Medicina Sperimentale e Scienze Biochimiche and INFM, Universitá di Roma Tor Vergata, Via di Tor Vergata 135, 00133 Roma, Italy, and Istituto di Medicina Sperimentale, CNR, Viale Marx 43, 00137 Roma, Italy, and Dipartimento di Chimica Biologica, Universitá di Padova, Viale G. Colombo 3, 35121 Padova, Italy

Received February 14, 2000; Revised Manuscript Received September 7, 2000

ABSTRACT: Among different proposed mechanisms to account for the protection exerted by estrogens against cardiovascular diseases, the antioxidant effect has attracted considerable attention. We confirmed that 17-β-estradiol (E2), when added to human LDL at a 6:1 ratio to apoB-100, markedly delays the phase of massive LDL lipid peroxidation induced by Cu^{2+}. We also observed an increased oxidative resistance of E2-treated LDL by monitoring the early phase of oxidative degradation on the basis of increased LDL surface polarity by the generalized polarization of the lipophilic fluorescent probe 2-(dimethylamino)-6-lauroylnaphthalene (Laurdan). A scavenging of free radicals by E2 is ruled out since, consistent with its structure, its rate constant for the reduction of peroxy radicals is extremely low, i.e., 0.02% of that of vitamin E. Tryptophan fluorescence lifetime and circular dichroism measurements revealed that (i) apoB-100 undergoes a conformational modification and a progressive loss of secondary structure during lipid peroxidation; (ii) E2 increases apoB-100 secondary structure and modifies its conformation; and (iii) the apoB-100 conformational change induced by E2 makes this protein resistant to modifications brought about by lipid peroxidation. We propose that E2, by affecting apoB-100 secondary structure and conformation, modifies the interaction of this protein with the outer layer of the LDL particle thus increasing its overall oxidative resistance.

Epidemiological data indicate that coronary heart disease is more prevalent in men and premenopausal women than in age-matched postmenopausal women. Estrogens that affect the plasma lipid profile (*1*) reduce the concentration of plasma homocysteine and angiotensin-converting enzyme (*2*, *3*), induce relaxation of the vasculature (*4*), and alter the level of clotting factors (*5*). The beneficial effect of estrogens on the oxidative stability of LDL is proposed to account for their anti-atherogenic effect (*6*−*10*), and 17-β-estradiol (E2)[1] appears the most active (*9*, *11*). E2 delays the oxidative modification of LDL both in vivo (*6*) and in vitro (*7*, *10*). Although hardly compatible with the molecular structure of E2, a peroxidation chain-breaking effect has been both proposed (*12*) and questioned (*13*) on the basis of the kinetics of its free-radical scavenging reaction. A recent report (*14*) shows that E2 prolongs the lag phase of LDL peroxidation and ascorbate increases dramatically the effect of E2. This synergism is unlikely due to a free-radical scavenging by E2, which, instead, would have produced an additive effect, thus prompting further investigation on the nature of the E2 antioxidant effect.

Using a 1:6 molar ratio between apoB-100 and E2 as the condition where the effect of E2 was maximal in the absence of ascorbate (*14*), we challenged LDL with Cu^{2+}, conditions widely used for testing oxidative resistance.

Our results provide evidence that the origin of the increased oxidative resistance conferred by E2 to LDL resides in a conformational change of apoB-100 that affects the interaction between apoB-100 and the lipidic surface of the LDL particle.

EXPERIMENTAL PROCEDURES

Measurement of E2 Antioxidant Capacity. E2 antioxidant capacity was determined by a competition kinetics method based on the inhibition of crocin bleaching in the presence of peroxy radicals (*15*), as modified by Tubaro et al. (*16*). Peroxy radicals were generated by thermal decomposition of 12.5 mM 2,2′-azobis-(2-amidinopropane)-dihydrocloride (ABAP) at 40 °C. The reaction mixture, equilibrated at 40

† This work was supported in part by the EU Biotechnology Project BIO4-CT97-2177 (T.P.).

* To whom correspondence should be addressed. Phone: (39 06) 86090-316. Fax: (39 06) 86090-332. E-mail: tiziana@biocell.irmkant.rm.cnr.it.

‡ I Clinica Ostetrica e Ginecologica.

§ Dipartimento di Medicina Sperimentale e Scienze Biochimiche and INFM.

|| Istituto di Medicina Sperimentale.

⊥ II Clinica Ostetrica e Ginecologica.

Dipartimento di Chimica Biologica.

[1] Abbreviations: ABAP, 2, 2′-azobis-(2-amidinopropane)-dihydrocloride; GP, generalized polarization; E2, 17-β-estradiol; Laurdan, 2-(dimethylamino)-6-lauroylnaphthalene; NATA, *N*-acetyl-tryptophanamide; POPOP, 2,2′-*p*-phenylene-bis-(5-phenyl)oxazole.

10.1021/bi000341p CCC: $19.00
Published on Web 10/21/2000

°C, contained 10 μM crocin in 0.1 M phosphate buffer, pH 7.0, 1% ethanol (vol %), 12.5 mM ABAP and different concentrations of Trolox C (5−25 μM), or E2 (50−250 μM). ABAP, Trolox C, and E2 were from Sigma Chemical Co. (St. Louis, MO). Crocin was purified from saffron flowers by washing with diethyl ether and extracting with methanol. The crocin concentration in methanol was determined by the absorbance at 443 nm using an extinction coefficient of 1.33×10^5 M^{-1} cm^{-1}.

LDL Purification and Peroxidation. Human LDL was isolated from healthy fasting volunteers by a short run ultracentrifugation procedure based on a nonequilibrium density-gradient using a Beckman L8−70M ultracentrifuge with a swinging bucket rotor SW41-TI (*17*). The isolated LDL fraction was dialyzed for 24 h against phosphate buffer, pH 7.4, that was deoxygenated by nitrogen bubbling. The protein concentration was adjusted to 0.1 μM of apoB-100 with phosphate buffer. The purity of the LDL preparation was checked by SDS gradient (3 to 15%) polyacrylamide gel electrophoresis under nonreducing conditions and stained with Comassie Brilliant Blue.

LDL samples (0.1 μM), in the absence or in the presence of E2 (0.6 μM), were peroxidized with 5 μM $CuSO_4$ at 37 °C. The peroxidation was stopped at various times with 50 μM ethylendiaminetetracetic acid, pH 7.4. Diene conjugation was measured by absorbance at 234 nm as previously described (*18*).

Laurdan Fluorescence. Samples of LDL suspension (1 mL, 0.1 μM), withdrawn after different times of incubation with Cu^{2+}, were labeled with 2-(dimethylamino)-6-lauroylnaphthalene (Laurdan, Molecular Probes Inc., Eugene, OR) by adding 0.3 μL of a 1.25 mM solution of the probe in dimethylsufoxide. The samples were equilibrated for 10 min at 37 °C in the fluorometer cell holder.

Laurdan generalized polarization (GP) measurements (*19*) were performed using a GREG 200 fluorometer (ISS Inc., Champaign, IL) equipped with a xenon arc lamp and photon counting electronics (PX01, ISS Inc.). The excitation was 360 nm with an 8 nm bandwidth. Emission spectra were acquired from 400 to 550 nm using an 8 nm bandwidth. Emission spectra were corrected for lamp intensity fluctuations. The cell holder was thermostatically maintained at 37.0 ± 0.1 °C using a circulating water bath. The GP value was calculated from the emission spectra according to

$$GP = (I_{440} - I_{490})/(I_{440} + I_{490}) \quad (1)$$

where I_{440} and I_{490} are the emission intensities at 440 and 490 nm, respectively (*19*).

Laurdan-labeled LDL samples under the different experimental conditions were also used for fluorescence lifetime measurements using a K2 phase fluorometer (ISS Inc.) equipped with a xenon arc lamp. An additional polarizer was inserted in the excitation light path, with an angle of 30°. Excitation was at 360 nm with a 16 nm bandwidth and the fluorescence was observed after a filter cutting below 418 nm. A solution of 2,2′−*p*-phenylene-bis-(5-phenyl)oxazole (POPOP) in ethanol was used as the reference (lifetime = 1.35 ns). The fluorometer cell holder was thermostatically maintained at 20.0 ± 0.1 °C, and the samples were continuously and mildly stirred. Phase and modulation data were acquired for 16 modulation frequencies, logarithmically spaced in the range from 9 to 200 MHz. Data were analyzed using the Globals Unlimited software (Laboratory for Fluorescence Dynamics, University of Illinois at Urbana−Champaign) using a Marquardt algorithm. The goodness of fit was evaluated by the value of the reduced chisquare (χ^2).

Tryptophan Fluorescence. The intensity variation of tryptophan residues fluorescence was measured at different times following addition of Cu^{2+}, with or without E2 at a molar ratio LDL:E2 of 1:6. The GREG 200 fluorometer was set at 295 ± 8 nm excitation and 330 ± 8 nm emission. The fluorometer cell holder was thermostatically maintained 37.0 ± 0.1 °C, and the samples were continuously stirred. Tryptophan fluorescence lifetime was measured in LDL by using the harmonic response technique, at 0.1 μM protein concentration. The excitation source was a frequency-doubled rhodamine dye laser pumped by a high repetition mode-locked Nd:YAG laser. The excitation wavelength was 295 nm and the emission was collected through a WG330 cutoff filter. The phase and modulation data were collected using the K2 fluorometer (ISS Inc.) and the accompanying software. The fluorometer cell holder was kept at 37 ± 0.1 or 20 ± 0.1 °C using a circulating water bath. During measurements, the samples were continuously mildly stirred. The data analysis was performed by the Globals Unlimited software using a Marquardt algorithm. The goodness of fit was evaluated on the basis of the value of the χ^2.

Circular Dichroism. Circular dichroism spectra of LDL (0.1 μM) under the different experimental conditions were recorded on a JASCO J-710 spectropolarimeter, using 0.1 cm quartz cuvette, in the peptidic region (200−250 nm). To increase the signal-to-noise ratio, six spectra were averaged for each measurement, and the blank was subtracted. The cell holder compartment was thermostatically maintained at 37 ± 0.1 °C using a circulating water bath. The spectra were analyzed for the content in α structure by using the software accompanying the spectropolarimeter.

RESULTS

The free-radical scavenging capacity of E2 was measured using a kinetic procedure based on the inhibition of the bleaching of the carotenoid crocin by thermally generated peroxy radicals. As expected on the basis of the E2 molecular structure, the relative rate constant of the reaction between E2 and peroxy radicals was quite low, accounting for only 0.02% of the antioxidant capacity of a chromanol bearing molecule such as Trolox C. Nevertheless, as measured by the formation of conjugated dienes, E2 increases the delay (lag phase) before the onset of the rapid phase of LDL peroxidation (Figure 1) from about 90 to 135 min. To explore the mechanism of this delay, we focused our investigations on this "lag phase". The Laurdan GP is extremely sensitive to variations in polarity occurring at the surface of lipid layers. In the presence of lipid oxidation products the Laurdan GP value increases (*20*−*22*). Indeed, Laurdan showed a surprising sensitivity to variations occurring in LDL lipids at early times after the oxidative stimulus. In LDL, the Laurdan GP value increased about 6% as early as 5 min after the addition of Cu^{2+}, reaching a plateau after 15 min with an increase of about 32% (Figure 1). In the presence of E2, a markedly slower increase of the GP value was observed, reaching the plateau after 60 min (Figure 1).

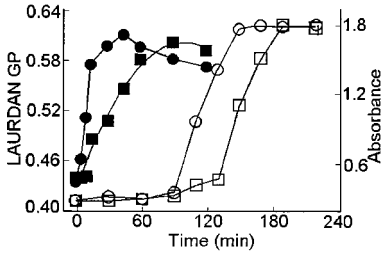

FIGURE 1: Laurdan GP and conjugated dienes in LDL incubated with Cu^{2+}. Laurdan GP values, measured at 37 °C, (filled symbols) and the absorbance of conjugated dienes (empty symbols), are plotted as a function of LDL incubation with Cu^{2+}, at 37 °C, in the presence (■, □) and in the absence (●, ○) of E2. Average results of five and three independent experiments, with standard deviation of 0.6 and of 3% for the GP and the diene conjugation, respectively.

Table 1: Laurdan Lifetime Values in LDL under the Different Experimental Conditions[a]

sample	C_1	F_1	W_1	C_2	F_2	W_2	χ^2	$\langle\tau\rangle$
control	6.67	0.57	2.26	1.20	0.43	3.78	1.15	4.32
+ Cu^{2+}	10.08	0.44	0.30	1.14	0.56	3.96	1.41	5.07
+ E2	7.57	0.47	1.84	1.39	0.53	3.54	1.20	4.29
+ Cu^{2+} + E2	9.92	0.46	0.29	1.03	0.54	3.63	1.41	5.12

[a] Results of a global fit of two independent measurements performed at 20 °C. The data have been analyzed following a model of two continuously distributed lifetime components, each with a center, C_i, a fractional amplitude, F_i, and a full width at half maximum, W_i. The average lifetime value is calculated by $\langle\tau\rangle = \sum_i C_i F_i$.

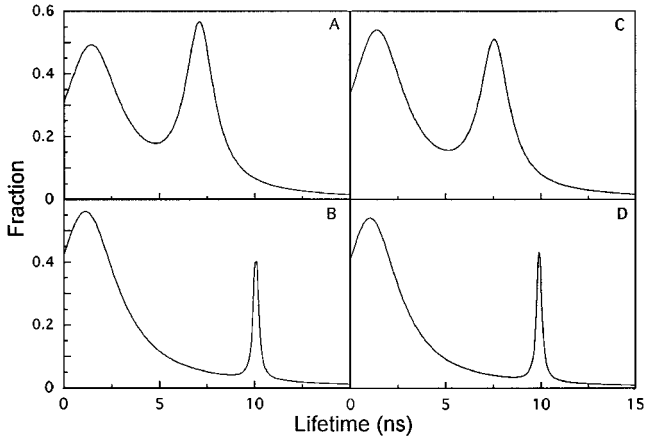

FIGURE 2: Laurdan lifetime distributions in LDL. Laurdan lifetimes measured at 20 °C in control LDL (A), after incubation for 1 h with Cu^{2+} (B and D), and in the presence of E2 (C and D). Results of a global fit of two independent experiments.

To rule out an increase of the GP value due to quenching of the probe emission (*23*) by lipid peroxidation products, we measured Laurdan fluorescence decay in LDL before and after incubation with Cu^{2+} for 60 min, when the GP value already reached a maximum both in the presence and in the absence of E2. A physical quenching would decrease the average lifetime value. The results, reported in the Table 1 and in the Figure 2, show that Laurdan decay in LDL is rather complex. As judged by the value of the χ^2 (Table 1), the phase and modulation data best fit a decay of two continuously distributed components with a Lorentzian shape. Each distributed component is characterized by a center value (*C*), a full width at half-maximum (*W*), and a fractional amplitude (*F*) (Table 1). In the presence of E2, only minor modifications of the Laurdan decay were observed (Figure 2, panels A and C), with an average lifetime ($\langle\tau\rangle$, Table 1) very close to that of the control. On the other hand, incubation of LDL with Cu^{2+} for 60 min deeply affected Laurdan decay even in the presence of E2 (Figure 2, panels B and D). In control and in E2-treated samples incubated with Cu^{2+} for 60 min, the calculated average lifetime increased (Table 1). Although small, this increase is sufficient to rule out a quenching of Laurdan fluorescence due to an interaction between the probe and lipid peroxidation products, and indicates, instead, that the increased GP value during incubation with Cu^{2+} was likely due to a relocation of the probe induced by the formation of hydrophilic domains in LDL, associated with the formation of lipid hydroperoxides, as will be discussed below.

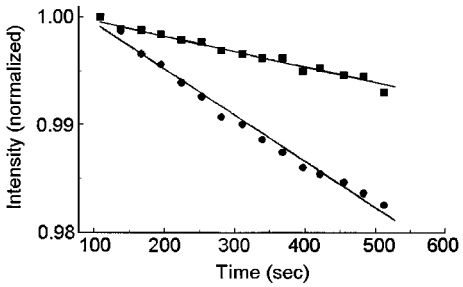

FIGURE 3: Tryptophan fluorescence intensity in LDL incubated with Cu^{2+}. Representative plot of the variation of tryptophan fluorescence intensity as a function of the incubation time of LDL with Cu^{2+}, in the presence (■) and in the absence (●) of E2. Time interval from 2 to 9 min. The initial intensity is normalized.

The intrinsic fluorescence intensity of tryptophan residues in apoB-100 was measured as a function of time following addition of Cu^{2+}. In agreement with previous reports (*24*), the tryptophan intensity decreased. In the Figure 3, the time course of this decrease is shown during the first 10 min after addition of Cu^{2+}. A slower decrease was observed in the presence of E2. The effect of Cu^{2+} on the intensity of the tryptophan molecule itself was tested by using a 10^{-5} M solution of *N*-acetyl-tryptophanamide (NATA) in PBS buffer. In the presence of Cu^{2+}, NATA intensity did not show any variation.

The fluorescence decay of the 37 tryptophan residues of the apoB-100 was measured, at 20 and at 37 °C. For measurements at 37 °C, the results are reported in Table 2 and in Figure 4. As expected, due to the presence of several tryptophan residues in various local microenvironments, the decay was quite complex. The phase and modulation data were fitted using different models of exponential and distributed decay functions, and the smallest value of the χ^2 was obtained for a model of two distributed lifetime components with a Lorentzian shape (Table 2). In control samples, the main component of the tryptophan decay (fraction = 0.64) is centered at 4.78 ns (Table 2 and Figure 4A). The residual fractional intensity (fraction = 0.36) originates from a component centered at 1.57 ns. Significant alterations of these decay components were observed both when the tryptophan lifetime of apoB-100 was measured in the presence of E2 and after incubation of LDL with Cu^{2+} for 60 min. The presence of E2 primarily affected the main component of the decay, with an increase of its center value and a decrease of its fractional intensity and width (Figure 4C). In the absence of E2, incubation of LDL with Cu^{2+} caused a decrease of the center value of both components

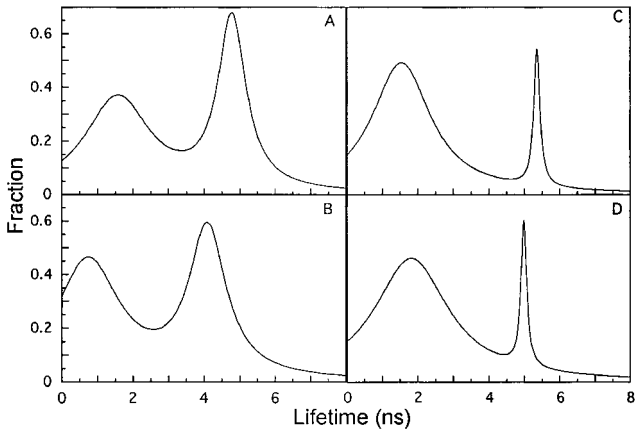

FIGURE 4: Tryptophan lifetime distribution in LDL. Measurements at 37 °C in control LDL (A), after incubation for 1 h with Cu^{2+} (B and D), and in the presence of E2 (C and D). Results of a global fit of two independent measurements.

of tryptophan decay and an increase in the fractional amplitude of the short lifetime component (Figure 4B). In agreement with the hypothesis of a quenching due to a higher exposure of tryptophan residues to water when LDL is oxidatively modified, the decrease of the tryptophan fluorescence intensity (Figure 3) fitted with the decrease of the calculated average lifetime value after incubation with Cu^{2+} (Table 2). The decay of the tryptophans in apoB-100, as modified by the presence of E2, was not further modified by incubation with Cu^{2+} (Figure 4, panel D in comparison with panel C). Similar results were obtained for measurements at 20 °C, although with higher average lifetimes (not shown). The effect of Cu^{2+} and of E2 on the decay of the tryptophan molecule itself was tested by using a 10^{-5} M solution of NATA in phosphate buffer. In either the presence of Cu^{2+} and/or E2, the NATA decay fitted a single discrete component with a lifetime of 2.84 ± 0.03 ns. A possible interference of vitamin E fluorescence with the tryptophan decay was also tested by measuring vitamin E lifetime in ethanol. Vitamin E decay resulted of a single discrete lifetime component with the value of 1.62 ± 0.03 ns. Considering that the molecular ratio between tryptophan and vitamin E in LDL is of more than 6 and that a direct relationship exists between the lifetime and the quantum yield, we evaluated that vitamin E contributes for a maximum of 6.5% to the total fluorescence emission. Previous steady-state evaluations (*25*) gave an even lower percentage of 2.7%. This low intensity of a discrete component cannot be resolved from the tryptophan lifetime distribution in either of our experimental conditions and does not interfere with the changes due to E2.

CD spectra of apoB-100, measured as a function of the incubation time with Cu^{2+}, in the absence or in the presence of E2, are reported in Figure 5. The percentage of α structure was of about 40%, in agreement with previous reports (*26*). When measured in the presence of E2 and in the absence of an oxidative stimulus, the CD spectrum of apoB-100 showed an increased secondary structure (Figure 5A) directly related to the concentration of E2. The plot of the CD signal of apoB-100 at a single wavelength (220 nm) and as a function of the incubation time with Cu^{2+} is reported in Figure 5B. An intensity decrease, indicating a progressive loss of secondary structure, was observed as a function of the incubation time with Cu^{2+} starting at intervals as early as 5 min. When LDL was incubated with Cu^{2+} in the presence of E2, only a minor decrease of the signal intensity could be observed (Figure 5B).

DISCUSSION

The peroxidation of LDL in the presence of transition metals depends on the concentration and availability of species such as lipid hydroperoxides (*27*), redox-labile amino acids in apoB-100 (*28*) and α-tocopherol (*29*), each of which can reduce the transition metal to its most reactive reduced form. Moreover, the plasma concentration of small-dense LDL has been suggested as a determinant of the peroxidability of the entire LDL fraction (*30*), among which is found the electronegative LDL (*31*). This suggests that, in addition to its antioxidant content, structural and physical elements can affect the oxidative stability of LDL. Calorimetry studies (*32*) provided evidence for a major effect on oxidative stability of order−disorder transitions of lipids in the surface monolayer. A modification of the lipid−protein interaction in LDL has been reported to decrease its oxidability (*33*), suggesting that the structure of LDL particles and particularly the features of the interaction between apoB-100 and lipids are a key element for its oxidative stability.

In agreement with previous reports (*7*, *14*, *34*) our data confirm that E2 delays the onset of the rapid phase of peroxidation of LDL. This effect of E2 cannot be accounted for by the reduction of peroxy radicals, the key reaction of chain-breaking antioxidants. The extremely low relative rate constant of E2 for the reduction of peroxy radicals (0.02% than that of Trolox C) is consistent with its molecular structure, where electron attracting substituents in the phenolic ring are missing and the transition to a stable quinone is not possible.

Variation of Laurdan GP in LDL during Cu^{2+}-mediated oxidation provides structural and kinetic information on the nature of changes occurring at the surface of LDL in the early phases after the application of the oxidative challenge. Laurdan is a membrane probe with virtually no affinity for proteins and with no appreciable fluorescence when in aqueous environments. As extensively reported, this probe is anchored by its lauric acid tail into the hydrophobic core of the membrane bilayer, with its polar naphthalene fluorescent moiety residing at the level of the glycerol backbone of phospholipids (*19*, *35*). Thus, following the currently accepted model for the structure of the lipids within the core and surface of LDL (*18*), Laurdan monitors the properties of the outer surface of the particle. The probe shows a red spectral shift as a function of increased polarity at the hydrophobic−hydrophilic interface (*19*, *20*). A blue emission is observed in nonpolar, gel-like, environments and a red emission is observed in more polar, liquid-crystalline-like, environments. In terms of GP values (eq 1), a blue emission gives high GP values and a red emission low GP values. Laurdan spectral changes have been observed after lipid peroxidation, where a blue spectral shift is directly related to the amount of peroxidation (*21*, *22*). Using phospholipid vesicles, a model has been proposed to explain this blue spectral shift (*21*, *22*). The main products of lipid peroxidation, i.e., hydroperoxide residues along the acyl chains, loosen the hydrophobic interactions between adjacent lipids,

Table 2: Fluorescence Lifetime of the 37 Tryptophan Residues in LDL under the Different Experimental Conditions[a]

sample	fitting function	C_1	W_1	F_1	C_2	W_2	F_2	χ^2	$\langle\tau\rangle$
control	1 exp	3.01		1.00				1322.4	
	2 exp	1.01		0.23	4.87		0.77	16.2	
	1 lor	3.28	3.42	1.00				22.4	
	2 lor	1.57	2.23	0.36	4.78	0.94	0.64	0.9	3.62
+ Cu^{2+}	2 lor	0.73	2.15	0.45	4.1	1.26	0.55	1.0	2.58
+ E2	2 lor	1.54	2.02	0.49	5.36	0.21	0.51	1.1	3.49
+ Cu^{2+} + E2	2 lor	1.82	2.53	0.46	4.99	0.19	0.54	0.9	3.53

[a] The control LDL sample has been analyzed using different fitting functions, following a model of one (1 exp) and two (2 exp) discrete components, and of one (1 lor) or two (2 lor) continuously distributed lifetime components with a Lorentzian distribution. The distributed decay components are characterized by a center, C_i, a full width at half maximum, W_i, and a fraction, F_i. Results of a global fit of two independent measurements performed at 37 °C. The average lifetime value is calculated by $\langle\tau\rangle = \sum_i C_i F_i$.

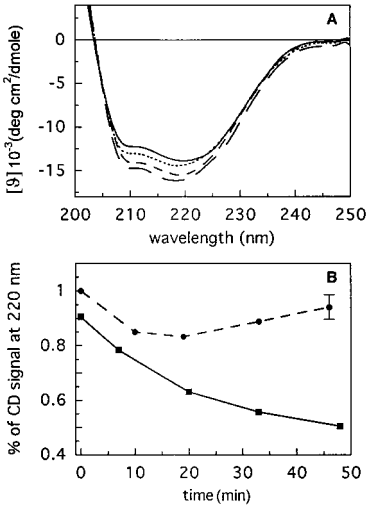

FIGURE 5: Circular dichroism of LDL. (A) Circular dichroism spectra of LDL (0.1 μM) measured at 37 °C in the absence (continuous line) and in the presence of different final concentrations of E2, of 0.25 (dotted line), 0.6 (dashed line) and 1 μM (long-dashed line). (B) Plot of the absorbance at 220 nm of the LDL circular dichroism spectra as a function of the incubation with Cu^{2+}, in the absence (■) and in the presence (●) of E2. Average results of three independent measurements. The error bar is reported at the 48 min point.

thus favoring the penetration of water into the lipid hydrophobic core down to the level of the hydroperoxide residues. Being hydrophobic, Laurdan relocates deeper into a more hydrophobic region of the lipids, giving a bluer emission spectrum and higher GP values (*20*−*22*). This model also fits the results obtained using the fluorescent membrane probe diphenylhexatriene in phospholipid vesicles (*20*, *21*) and in cell membranes (*36*) that contain increasing concentrations of hydroperoxides. The reported changes of Laurdan lifetime value after Cu^{2+}-induced lipid peroxidation excludes any direct interaction between the probe and oxidation products (*23*). Here, we detected a linear increase of the GP value during the early phase of the Cu^{2+}-induced peroxidation. We attribute this GP increase to an increased water concentration in the surface of the LDL particle, due to the increased concentration of lipid peroxidation products. This surface hydration of LDL occurs at early times after the Cu^{2+}-induced peroxidation and the Laurdan GP increases without a lag phase. Instead, the increase of conjugated diene absorbance started after a lag phase of about 100 min after the addition of Cu^{2+} (Figure 1). This result is not surprising when considering that Laurdan detects minute concentrations of hydroperoxides and that diene conjugation absorbance is a method with a rather low sensitivity for measuring lipid peroxidation products. Therefore, the results obtained by Laurdan GP indicate that the oxidative damage to lipids in LDL is occurring almost immediately after the addition of Cu^{2+}, without a lag phase, and that the structural consequence of this accumulation of lipid peroxidation products is a decreased packing of the surface lipids, accompanied by an increased water concentration. In the presence of E2, this initial phase of peroxidation is much slower, indicating that E2 affects the oxidative events leading to the perturbation of the surface of LDL through a modification of apoB-100, i.e., through a modification of the interaction between this protein and the surface lipids.

An increased hydration of the LDL surface due to lipid peroxidation is in agreement with the results obtained by tryptophan fluorescence intensity and lifetime. Indeed, the fluorescence of tryptophan residues can be quenched by a local increase in water concentration (*38*, *39*). We observed that tryptophan fluorescence intensity (Figure 3) and lifetime values (Figure 4 and Table 2) decreased after LDL incubation with Cu^{2+}. Tryptophan fluorescence is extremely sensitive to changes in its local microenvironment which, in turn, changes for protein conformational modifications (*37*, *38*). Thus, the measurement of tryptophan lifetimes provides information on variations in protein tertiary structure. In proteins containing several tryptophan residues, the best description of the decay has been obtained using a model of continuously distributed lifetime components, successfully applied to the study of the tertiary structure of several proteins (*39*−*41*). In apoB-100, the 37 tryptophans yield a complex decay described by two continuously distributed lifetime components, each with a relatively large width. After incubation with Cu^{2+}, the shift of both tryptophan lifetime components toward shorter values and the increase of the relative fraction of the shortest component were evident. Also, the calculated average lifetime decreases, in agreement with an increased exposure of several tryptophans to the aqueous environment. Neither the steady-state intensity nor the lifetime of NATA were modified by incubation with Cu^{2+}, and the observed modification of tryptophan decay in apoB-100 cannot be attributed to a direct oxidation of this residue by Cu^{2+}. In part, some tryptophan residues can be also oxidatively bleached. Nevertheless, after oxidative modification of LDL, apoB-100 tryptophan fluorescence originates from residues with an increased exposure to water. In addition, a partial tryptophan oxidation does not influence our major conclusion about the conformational modification of apoB-100 due to E2 and of a virtually nil further

conformational modification at longer times, when lipids are oxidized.

Consistent with the Laurdan GP data, the loss of secondary structure of apoB-100 detected by circular dichroism also started almost immediately after addition of Cu^{2+} with no lag phase before the massive lipid peroxidation corresponding to the propagation phase. Minute amounts of lipid hydroperoxides that modify the packing of the LDL surface lipids, with an increased local hydration, also modify the interaction between the apoB-100 and the surface lipids in such a way that the protein's secondary structure decreases.

E2 induces relevant secondary and tertiary conformational modifications to apoB-100 and makes this protein resistant to further modifications due to Cu^{2+}-induced peroxidation. In the absence of an oxidative challenge, E2 modifies both components of the tryptophan fluorescence decay. Although the average tryptophan lifetime value did not show appreciable differences in the presence of E2, the center and the fractional intensity of the individual components of the tryptophan decay were modified. In particular, the increased value of the long lifetime component (Figure 4, panels A and C), together with the CD data showing an increased secondary structure (Figure 5A), suggests that E2 induces an increased conformational packing of apoB-100. This conformation is particularly resistant to perturbations related to Cu^{2+}-induced peroxidation. By causing a more stable protein conformation, E2 prevents the peroxidation-induced apoB-100 unfolding. This more stable conformation appears to be responsible for the increased resistance to lipid peroxidation (Figure 1).

The molar ratio between apoB-100 and E2 was as low as 1:6, and the ratio between LDL lipids and E2 is in the range of 500:1−750:1, based on the apoB-100 and lipid content of LDL. Thus, the E2 effect cannot be attributed to a modification of lipid packing as, for instance, is the case when the concentration of cholesterol in membranes increases. Indeed, the minimum cholesterol to total lipid ratio required to produce a detectable change in membrane lipid packing is 1:20 (*42*). This supports the concept that E2 affects apoB-100 conformation directly and not through changes in the lipid moiety of LDL. Although E2 belongs to a family of steroid hormones with similar chemical structure, other steroid hormones do not afford a protection against Cu^{2+}-induced LDL peroxidation (*43*).

ACKNOWLEDGMENT

We thank Fabio De Matteis for his technical assistance at the L.A.S.P. (Laboratorio di Spettroscopia al Nanosecondo) facility at the University of Rome, Tor Vergata.

REFERENCES

1. Walsh, B. W., Schiff, I., Rosner, B., Greenberg, L., Ravnikar, V., and Sacks, F. M. (1991) *N. Engl. J. Med. 325*, 1196−1204.
2. Lien, E. A., Anker, G., Lonnig, P., Refsum, H., and Veland, P. M. (1997) *Biochem. Soc. Trans. 25*, 33−35.
3. Proudler, A. J., Ahmed, A. I., Crook, D., Fogelman, I., Rymer, J. M., and Stevenson, J. C. (1995) *Lancet 346*, 89−90.
4. Garyac, K. F., Vyas, J., and Whitehead, M. (1991) *Lancet 338*, 839−842.
5. Lindoff, C., Peterson, F., and Lecander, J. (1993) *Maturitas* 17, 17−22.
6. Sack, M. N., Rader, J., and O'Cannon, R. (1994) *Lancet 343*, 269−270.
7. Shawaery, G. T., Vita, J. A., and Keaney, J. F. (1997) *Circulation 95*, 1378−1385.
8. Huber, L., Scheffer, E., Poll, T., Ziegler, R., and Dresel, H. (1990) *Free Radical Res. Commun. 8*, 167−173.
9. Rifici, V., and Khachadurian, A. (1992) *Metabolism 41*, 110−1114.
10. Ayres, S., Yang, M., and Ravi Subbiah, M. T. (1996) *J. Lab. Clin. Med. 128*, 367−375.
11. Moorodian, A. D. (1993) *J. Steroid Bioch. Mol. Biol. 45*, 509−511.
12. Liu, G. T., Zhary, T. M., Wary, B. E., and Wary, J. W. (1992) *Biochem. Pharmac. 43*, 147−152.
13. Niki, E., and Nakano, M. (1990) *Methods Enzymol. 186*, 330−333.
14. Hwang, J., Peterson, H., Hodis, H., Choi, B., and Sevanian, A. (2000) *Atherosclerosis* (in press).
15. Bors, W., Michel, C., and Saran, M. (1984) *Biochim. Biophys. Acta 796*, 312−319.
16. Tubaro, F., Micossi, E., and Ursini, F. (1996) *J. Am. Oil Chem. Soc. 73*, 173−179.
17. Chapman, M. J., Laplaud, P. M., Luc. G., Forgez, P., Bruckert, E., Goulinet, S., and Lagrange, D. (1988) *J. Lipid Res. 29*, 442−458.
18. Esterbauer, H., Gebicki. J., Puhl, H., and Jürgens. G. (1992) *Free Radicals Biol. Med. 13*, 341−390.
19. Parasassi, T., De Stasio, G., d'Ubaldo, A., and Gratton, E. (1990) *Biophys. J. 57*, 1179−1186.
20. Parasassi, T., Giusti, A. M., Gratton, E., Monaco, E., Raimondi, M., Ravagnan, G., and Sapora, O. (1994) *Int. J. Radiat. Biol. 65*, 329−334.
21. Parasassi, T., Giusti, A. M., Raimondi, M., Ravagnan, G., Sapora, O., and Gratton, E. (1995) *Free Radicals Biol. Med. 19*, 511−516.
22. Kivatinitz, S. C., Pelsman, M. A. Alonso A. d. C., Bagatolli, L., and Quiroga, S. (1997) *J. Neurochem. 69*, 2102−2114.
23. Parasassi, T., Ravagnan, G., Rusch, R. M., Gratton, E. (1993) *Photochem. Photobiol. 57*, 403−410.
24. Reyftmann, J., Santus R., Maziere J., Morliere P., Salmon S., Candide C. Maziere C., and Haisle J. (1990) *Biochim. Biophys. Acta 1042*, 159−167.
25. Giessauf, A., Steiner, E., Esterbauer H. (1995) Early destruction of tryptophan residues of apolipoprotein B is a vitamin E-independent process during copper-mediated oxidation of LDL. *Biochim. Biophys. Acta 1256*, 221−232.
26. Lund-Katz, S., Laplaud, P. M., Phillips, M. C., and Chapman, M. J. (1998) *Biochemistry 37*, 12867−12874.
27. Patel, R., Svistunenko, D., Wilson, M. T., and Darley-Usmar, V. (1997) *Biochem. J. 322*, 425−433.
28. Giessauf, A., Steiner, E., and Esterbauer, H. (1995) *Biochim. Biophys. Acta 1256*, 221−232.
29. Kontush, A., Meyer, S., Finckh, B., Kohlschutter, A., and Beisiegel, U. (1996) *J. Biol. Chem. 271*, 11106−11112.
30. Sevanian, A., Hwang, J., Hosis, H., Cazzolato, G., Avogaro, P., and Bittolo-Bon, G. (1996) *Arteriscler. Thromb. 16*, 773−783.
31. Sevanian, A., Bittolo-Bon, G., Cazzolato, G., Hodis, H., Hwang, J., Zamburlini, A., Maiorino, M., and Ursini, F. (1997) *J. Lipid Res. 38*, 419−428.
32. Schuster, B., Prassl, R., Nigon, F., Chapman, M. J., and Laggener, P. (1995) *Proc. Natl. Acad. Sci. U.S.A. 92*, 2509−2513.
33. Abuja P. M., Lohner K., and Prassl R. (1999) *Biochemistry 38*, 3401−3408.
34. McManus, J., McEneny J., Thompson W., and Young I. S. (1997) *Atherosclerosis, 135*, 73−81.
35. Bagatolli, L. A., Parasassi, T., Fidelio G. T., and Gratton, E. (1999) *Photochem. Photobiol. 70*, 557−564.
36. Giusti, A. M., Raimondi, M., Ravagnan, G., Sapora O., and Parasassi, T. (1998) *Int. J. Radiat. Biol. 74*, 595−605.
37. Burstein, E. A., Vedenkina, N. S., and Ivkova, M. N. (1973) *Photochem. Photobiol. 18*, 263−279.

38. Beechem, J. M., and Brand, L. (1985) *Annu. Rev. Biochem. 54*, 43−71.
39. Rouviere, N., Vincent, M., Craescu, C. T., and Gallay, J. (1997) *Biochemistry 36*, 7339−7352.
40. Di Venere, A., Mei, G., Gilardi, G., Rosato, N., De Matteis, S., MacKay, R., Gratton, E., and Finazzi-Agró, A. (1998) *Eur. J. Biochem. 257*, 337−343.
41. Garcia, P., Mérola, F., Receveur, V., Blandin, P., Minard, P., and Desmadril, M. (1998) *Biochemistry 37*, 7444−7455.
42. Parasassi, T., Di Stefano, M., Loiero, M., Ravagnan, G., and Gratton, E. (1994) *Biophys. J. 66*, 120−132.
43. Shawaery, G. T., Vita, J. A., and Keaney, J. F. (1998) *Atherosclerosis 138*, 255−262.

BI000341P